Available online at www.sciencedirect.com
ScienceDirect
Applied Surface Science 254 (2008) 2325–2330
applied surface science
www.elsevier.com/locate/apsusc

The role of halide ions on the electrochemical behaviour of iron in alkali solutions

S. Nathira Begum *, V.S. Muralidharan, C. Ahmed Basha

Central Electrochemical Research Institute, Karaikudi 630006, India

Received 7 May 2007; received in revised form 18 August 2007; accepted 10 September 2007
Available online 14 September 2007

Abstract

Active dissolution and passivation of transition metals in alkali solutions is of technological importance in batteries. The performance of alkaline batteries is decided by the presence of halides as they influence passivation. Cyclic voltammetric studies were carried out on iron in different sodium hydroxide solutions in presence of halides. In alkali solutions iron formed hydroxo complexes and their polymers in the interfacial diffusion layer. With progress of time they formed a cation selective layer. The diffusion layer turned into bipolar ion selective layer consisted of halides, a selective inner sublayer to the metal side and cation selective outer layer to the solution side. At very high anodic potentials, dehydration and deprotonation led to the conversion of salt layer into an oxide.

Keywords: Cyclic voltammetry; Iron dissolution; Passivation; Halide ions

1. Introduction

Active anodic dissolution and passivation of iron in alkali solution is of technological importance in view of the fact that iron is used as the anode in Ni/Fe, Fe/air batteries and a class of batteries, referred to as super-iron batteries, containing a cathode utilizing a common material (iron) in an unusual (greater than 3) valence state [1,2]. The cathode is based on abundant starting materials, and is compatible with an alkaline electrolyte, and either a zinc or a metal hydride anode. The improved high specific charge capacity of metal hydride anodes is greater than that of the nickel oxyhydroxide cathode in metal hydride batteries. Similarly, the high specific charge capacity of zinc anodes is greater than that of the manganese dioxide cathode in alkaline batteries. The storage capacity in both of these batteries is significantly cathode limited. Replacement of the manganese dioxide or nickel oxyhydroxide cathodes in these cells with a more energetic cathode such as ferrate (Fe(VI)) compounds can substantially increase the energy storage capacity of these cells. For example, using the same zinc anode and electrolyte, Fe(VI) cathode batteries were shown to provide 50% more energy capacity than in conventional alkaline batteries [3,4]. Yet another driving force behind these studies has been to expand the fundamental understanding of the aqueous chemistry of non-heme hypervalent iron complexes [5]. The anodic reaction in the active range is the formation of $Fe(OH)_2$, FeOOH and as the potential becomes more positive it goes directly into the hexavalent ferrate state. Ferrate provides a convenient entry into hypervalent iron chemistry since it must go through the +5 or +4 oxidation state during its reduction. This work has important applications in the fields of bioinorganic chemistry and iron-catalyzed organic oxidations, e.g. O_2 and Fenton-like systems. Each of these areas now invokes iron(IV) and iron(V) reaction intermediates [6].

Many studies about active dissolution and passivation were carried in alkaline solution [7–16] and many electrochemical studies have been investigated the behaviour of iron in aqueous solution. Several mechanism have been suggested [7–13] but no consensus has yet been found been different authors. However, the majority of authors propose the existence of an intermediate transient species Fe(I) generally designated as $FeOH_{ads}$ although there is little, if any, direct evidence for its existence [8,17,18]. In the presence of a sufficient quantity of OH^- and/or an aggressive anion, A^-, competitive adsorption between water molecules and anions may occur, which means that surface

---

* Corresponding author. Tel.: +91 4565 227550; fax: +91 4565 227713.
E-mail address: nava_572004@yahoo.co.in (S.N. Begum).

0169-4332/$ – see front matter © 2007 Elsevier B.V. All rights reserved.
doi:10.1016/j.apsusc.2007.09.019

attack occurs by forming $Fe[H_2O]$ or $Fe(A^-)$ groups [8]. If A^- forms an iron soluble salt, the corrosion is not uniform but if the salt is insoluble A^- may assist passivation, depending on its capacity for homogeneously covering the metallic surface increasing the ionic charge transfer resistance [8]. The species $Fe[H_2O]$ or $Fe(OH^-)$ initiate the oxidation process by electrochemical deprotonation reactions [8,9,18].

Under potentiodynamic conditions, the first anodic peak is specifically related to $Fe(OH)_2$ formation and the second peak to $Fe(OH)_2$ with three-dimensional oxide film and the third peak to FeOOH formation [19–21]. From the variation of the peak height as a function of sweep rate and hydroxide concentration [22] the film growth on the surface was assigned to low field migration of ions through an oxide/hydroxide lattice. Again the three anodic peaks observed [23,24] had been assigned to the ionization of adsorbed hydrogen, $Fe(OH)_2$ and Fe_3O_4 formation.

It is to be noted that in literature, from measurements of kinetic data obtained using an iron rotating disk electrode by cyclic voltammetry under quasi-steady-state conditions with compensation of the ohmic drop, proposed the following dissolution mechanism as shown below:

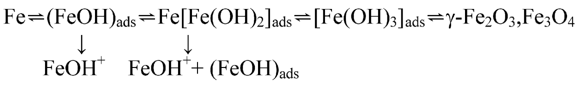

$$\begin{array}{l}\mathrm{Fe}\rightleftharpoons(\mathrm{FeOH})_{ads}\rightleftharpoons\mathrm{Fe[Fe(OH)_2]}_{ads}\rightleftharpoons[\mathrm{Fe(OH)_3}]_{ads}\rightleftharpoons\gamma\text{-}\mathrm{Fe_2O_3},\mathrm{Fe_3O_4}\\ \qquad\quad\downarrow\qquad\qquad\quad\downarrow\\ \qquad\mathrm{FeOH^+}\qquad\mathrm{FeOH^+}+(\mathrm{FeOH})_{ads}\end{array}$$

This iron dissolution kinetics was found to be independent of the anion concentration in the overall potential range. Cyclic voltammetric studies carried out by several authors for iron in alkaline solutions had an overall agreement in the formation of two peaks [19,20] in the cathodic scan while it is not so in the anodic scan. Some authors reported three peaks and others only two peaks. This variation arises mainly due to experimental conditions. Influence of halides on the electrochemical behaviour of iron in alkali solutions is of technological and basic interest as the halides influence the performance of alkaline batteries.

In the present study cyclic voltammetric studies were carried out in alkali solutions to understand the influence of halides on the dissolution and passivation iron.

2. Materials and methods

The experimental set up is shown in Fig. 1. The working electrode was made of pure iron rod (99.9999% purity, Johnson Matthey Chemicals Ltd., UK) with a circular area of 0.2 cm^2. The rod was embedded in Teflon gaskets and electrical connections were provided by screw and thread arrangement. The surface of the electrode was polished successively with finest grade emery papers and with 0.05 μm alumina, degreased with trichloroethylene and washed with running double distilled water. The counter electrode was a platinum sheet of 4 cm^2 area and a $Hg/HgO/OH^-$ ion electrode was used as reference. A potentiostat/galvanostat Model IM6 was used for obtaining cyclic voltammograms (CVs).

Analar grade reagents and triple distilled water were used. The experiments were carried out in 0.1, 1.0 and 5 M NaOH (analar grade, Ranbaxy, India) solutions with the introduction of different amounts of halide salts (analar grade, Ranbaxy, India) to get predetermined concentrations of halides (Cl^-, Br^- and I^-) in alkali solution. That is the required amount of halides salt was added to 0.1 and 1.0 M NaOH solution (see Table 1) to reach halide ion concentration as 0, 0.005, 0.01 and 0.05 M where as in case of 5 M NaOH solution halide salts were introduced to get its concentration as 0, 0.25, 0.5 and 2.5 M. All solutions were deoxygenated with purified nitrogen. Each experiment was performed with freshly prepared solutions and on freshly prepared surface. All measurements were performed at $30 \pm 1\ ^\circ C$.

The potentiodynamic polarization curves were recorded by changing the potential automatically at the desired sweep rate. In order to start with a clean surface, the electrode was kept at −1.3 V for half an hour, disconnected shaken free of adsorbed hydrogen and then subjected to triangular potential scan at various sweep rates.

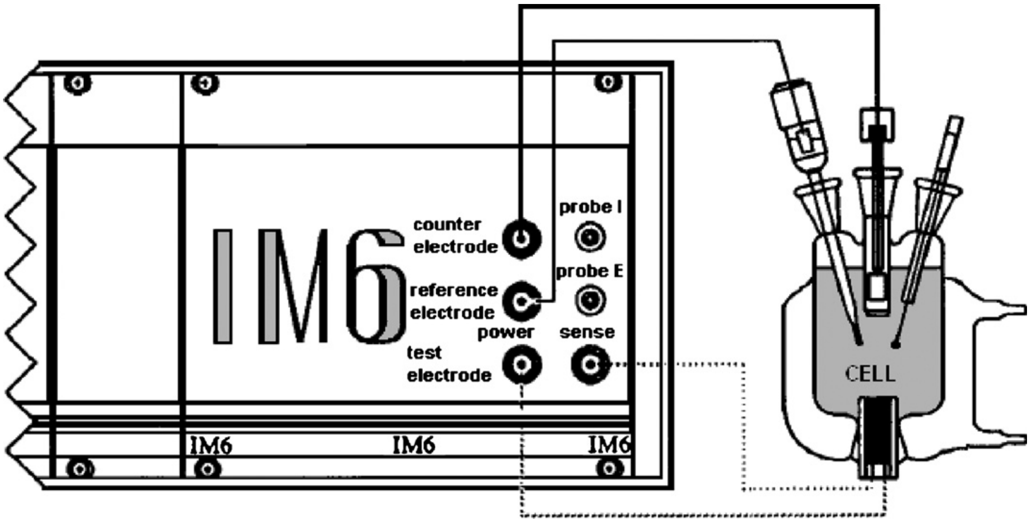

Fig. 1. Experimental set up.

Table 1
Various peak potentials of the CVs of pure iron in 0.1, 1.0 and 5.0 M NaOH in presence and absence of halide ion

CV	Anodic (forward scan)				Cathodic (reverse scan)		
	P(I)	P(II)	BS	ZCCP	P(III)	P(IV)	P(V)
0.1 M NaOH	−955 mV Fe → $FeOH_{ads}$	−592 mV $FeOH_{ads}$ → $Fe(OH)_2$ → $Fe(OH)_3$	−430 to −260 mV oxide thickening	−480 mV	−694 mV Fe(III) → Fe(II)	−1030 mV Fe(II) → Fe H_2 evolution	−1259 mV H_2 evolution
+5 mM chloride	−952 mV	−601 mV	−300 mV	−508 mV	−691 mV	−1049 mV	−1261 mV
+5 mM bromide	−955 mV	−600 mV	–	−531 mV	−1049 mV	−1259 mV	–
+5 mM iodide	−950 mV	−600 mV	–	−500 mV	−1030 mV	−1259 mV	–
1.0 M NaOH	−1000 mV Fe → Fe $(OH)_{ads}$	−604 mV $FeOH_{ads}$ → $Fe(OH)_2$ → $Fe(OH)_3$	–	−502 mV	−1033 mV Fe(III) → Fe(II)	−1180 mV Fe(II) → Fe H_2 evolution	–
+5 mM chloride	−990 mV	−618 mV	–	−505 mV	−1036 mV	−1180 mV	–
+5 mM bromide	−985 mV	−613 mV	–	−385 mV	−1028 mV	−1180 mV	–
+5 mM iodide	−987 mV	−613 mV	–	−493 mV	−1042 mV	−1180 mV	–
5.0 M NaOH	−612 mV $FeOH_{ads}$ → $Fe(OH)_2$ → $Fe(OH)_3$	–	–	−400 mV	−1036 mV Fe(III) → Fe(II)	−1181 mV Fe(II) → Fe H_2 evolution	–
+50 mM chloride	−629 mV	–	–	−400 mV	−1066 mV	−1213 mV	–
+50 mM bromide	−800 mV	−650 mV	–	−400 mV	−1075 mV	−1200 mV	–
+50 mM iodide	−900 mV	−625 mV	–	−400 mV	−1075 mV	−1210 mV	–

The potential range −1300 mV ($E_{\lambda c}$) to +100 mV ($E_{\lambda a}$) was fixed at a sweep rate of 100 mV s^{-1} after several experiments to get reproducible *E*–*i*.

3. Results and discussions

The results of all the experiments carried out were presented in Figs. 2–7, Tables 1 and 2.

3.1. Electrochemical behaviour in NaOH solutions containing halide ions

Fig. 2 illustrates the CVs a, b, c and d of pure iron in 0.1 M NaOH containing halide ion. In absence of the halide ions, the CV is represented by ‘a’ which is when polarized from −1300 to 100 mV at fixed sweep rate of 100 mV s^{-1}. In the forward scan the anodic peak (I) is exhibited at −955 mV and it is followed by a second peak (II) at −592 mV. A broad shoulder was observed in the range of −430 to −260 mV. While reversing the scan zero current crossing potential (ZCCP) was seen at −480 mV. Cathodic peak (III), peak (IV) and peak (V) were appeared at −694, −1030 and −1259 mV, respectively.

Introduction of chloride ions did not greatly modify the electrochemical spectrum. In presence of 5 mM chloride solutions anodic peaks were seen at −952, −601 mV followed by a shoulder at −300 mV. While reversing the scan, ZCCP occurred at −508 mV followed by cathodic peaks at −691, −1049 and −1261 mV.

Increase of chloride ions concentration did not affect anodic peak potentials. ZCCP became active while cathodic peak potentials became nobler suggesting that the presence of chloride in solution favoured reduction. Anodic and cathodic

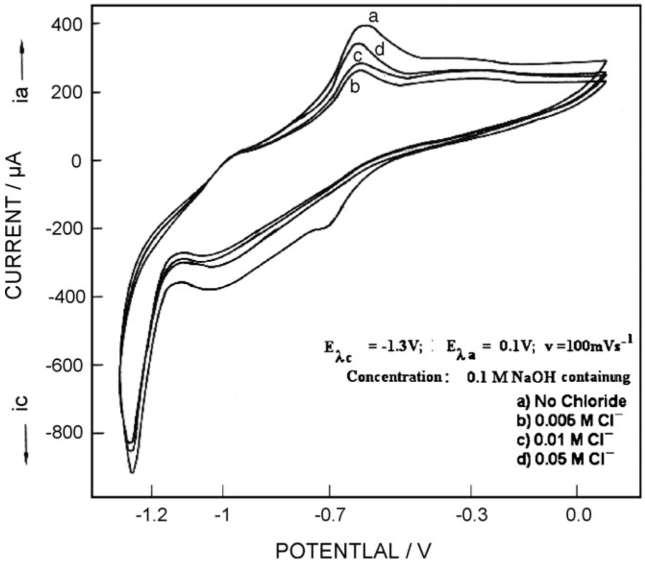

Fig. 2. Cyclic voltammograms for iron in 0.1 M NaOH solution containing different amounts of chloride.

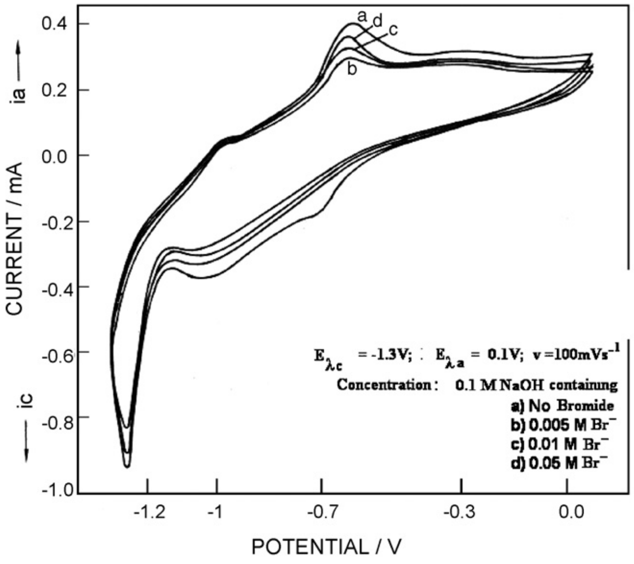

Fig. 3. Cyclic voltammograms for iron in 0.1 M NaOH solution containing different amounts of bromide.

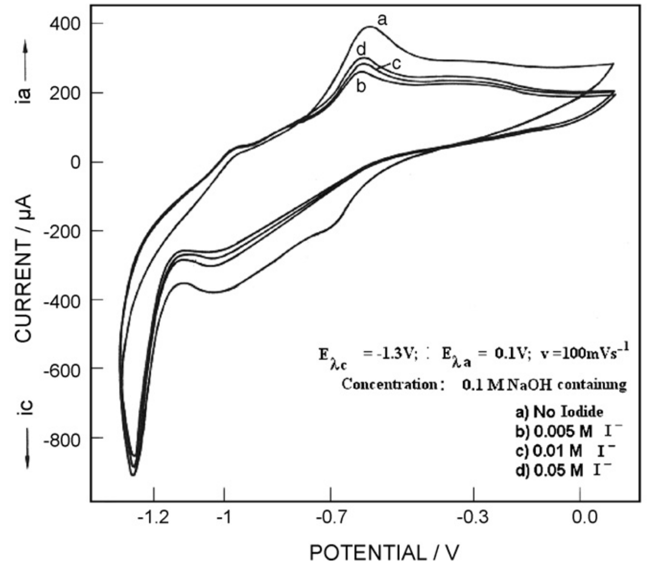

Fig. 4. Cyclic voltammograms for iron in 0.1 M NaOH solution containing different amounts of iodide.

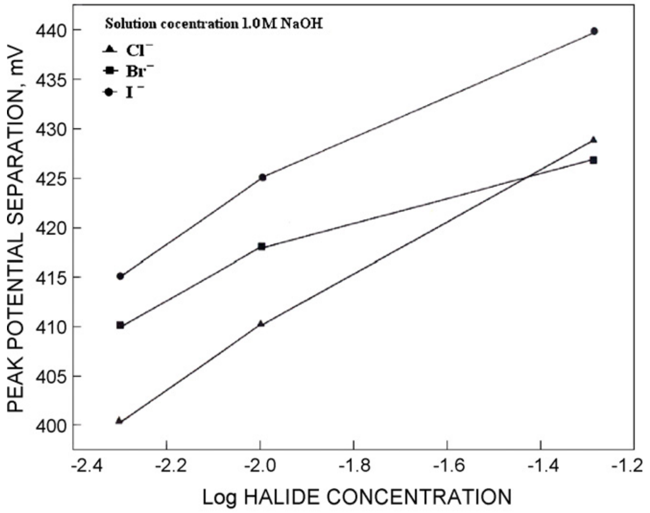

Fig. 6. Variation of peak potential separation with log halide concentration in 1.0 M NaOH solution.

peak currents increased with chloride ion concentration as shown by the CVs b, c and d in Fig. 2.

Fig. 3 presents the electrochemical spectrum observed in presence of bromide ion concentrations. In 5 mM bromide solutions, anodic peaks appeared at −955 mV (I) and −600 mV (II), while reversing the scan ZCCP occurred at −531 mV. Two cathodic peaks were observed at −1049 and −1259 mV. Increase of bromide ion concentration did not affect anodic peak potentials, cathodic peak potentials became active. Increase of bromide ion concentration increased peak currents.

Introduction of iodide ions (Fig. 4) did not modify the electrochemical spectrum. When polarized from −1300 mV in presence of 5 mM the forward scan exhibits anodic peaks at −950 and −600 mV. While reversing the scan ZCCP appeared at −500 mV. Cathodic peaks were seen at −1030 and −1259 mV. Increase of iodide ion concentration caused anodic peak potentials to become nobler and cathodic peak potentials to become active. Anodic and cathodic peak currents increased with iodide ion concentration. In 50 mM iodide ion concentration an anodic additional peak was seen at −800 mV.

Table 2 presents the various peak potentials of the CVs of pure iron in 0.1, 1.0 and 5.0 M NaOH in presence and absence of halide ion which is when polarized from −1300 to 100 mV at fixed sweep rate of 100 mV s^{-1}.

In the present study, in 0.1 M NaOH solutions the observed anodic peak at the value of −955 mV is due to the oxidation of Fe to $FeOH_{ads}$. The second anodic peak at −592 mV is due to the oxidation of $FeOH_{ads} \rightarrow Fe(OH)_2 \rightarrow Fe(OH)_3$ and the shoulder around −430 mV is due to the thickening of the oxide. During the reverse scan the observed cathodic peak at −694 mV is due to the reduction Fe(III) → Fe(II). The cathodic peaks at −1030 and −1259 mV are due to the reduction of Fe(II) → Fe followed by hydrogen evolution.

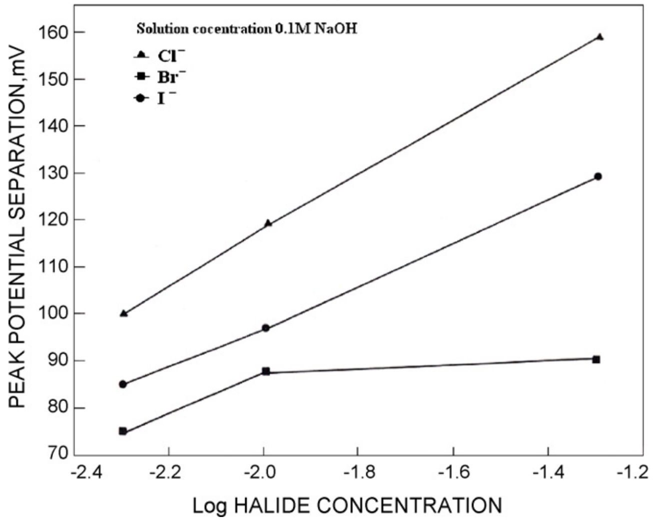

Fig. 5. Variation of peak potential separation with log halide concentration in 0.1 M NaOH solution.

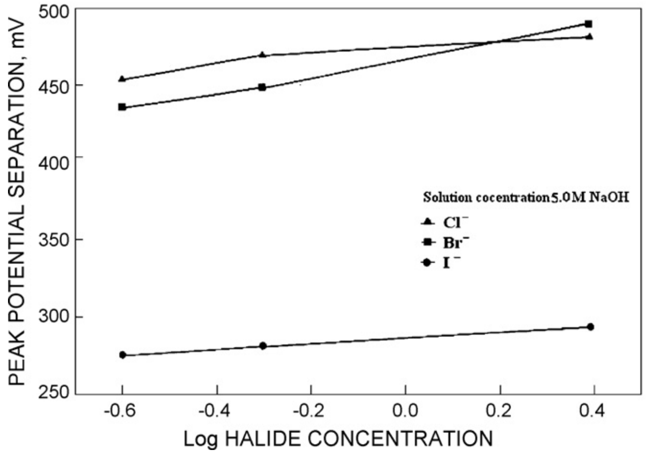

Fig. 7. Variation of peak potential separation with log halide concentration in 5.0 M NaOH solution.

Table 2
Variation of second anodic peak currents (mA) with halide ion concentrations

[NaOH] (M)	[X^-] (M)	Second anodic peak currents (mA)		
		Chloride	Bromide	Iodide
0.1	0	0.367	0.367	0.367
	5×10^{-3}	0.244	0.308	0.214
	10^{-2}	0.255	0.312	0.23
	5×10^{-2}	0.316	0.344	0.24
1.0	0	1.51	1.51	1.51
	5×10^{-3}	1.25	0.75	1.35
	10^{-2}	1.27	1.4	1.40
	5×10^{-2}	1.29	1.50	1.45
5.0	0	2.2	2.2	2.2
	2.5×10^{-1}	1.9	0.4	1.8
	5×10^{-1}	2.1	0.8	2.0
	2.5	2.1	2.0	2.2

In 1.0 M alkali solutions the observed anodic peaks at −1000 and −604 mV are due to Fe → $FeOH_{ads}$ followed by its conversion to $Fe(OH)_2$. The observed cathodic peaks at −1033 mV are due to conversion of Fe(III) → Fe(II), Fe(II) → Fe is followed by hydrogen evolution.

In 5.0 M NaOH solutions the observed anodic peak at −612 mV is due to the formation of Fe(II) species which gets oxidized at higher potentials. The cathodic peaks at −1036 mV is due to the direct reduction of Fe(III) → Fe(II), Fe(II) → Fe, followed by hydrogen evolution. The appearance of an anodic peak at −600 mV is due to the formation of $Fe(OH)_2$.

The measured charges on anodic and cathodic peaks indicated the formation and reduction of multilayer oxide films. Oxidation and reduction processes taking place on an iron electrode and the cyclic voltammetric behaviour can be viewed as follows. The first anodic peak can more probably be assigned to oxidation of iron as Fe → $FeOH_{ads}$ [25,26] than to oxidation of adsorbed hydrogen [27–29]. The second anodic peak corresponds to the reaction Fe → $Fe(OH)_2$. The third anodic peak may be related to oxidation of both Fe to Fe(II) and Fe(II) to Fe(III) [25], on considering the anodic charge flowing under the peak. The hump which was observed at more anodic potentials than the third anodic peak can be related to thermodynamically more stable Fe(III) species than that formed in the peak.

X-ray diffraction studies on oxide of iron [30] revealed that γ-Fe_2O_3 to be present in all passive films independent of pH. The films formed in the prepassive and trans passive regions contained the Fe_3O_4 spinal structure and not γ-Fe_2O_3. Ellipsometric responses of iron electrode in alkali showed a composite structure of the passivating layer involving an inner layer which was difficult to reduce electrolytically, probably related to Fe_3O_4 and an outer gelatinous iron hydroxide which is reducible [31]. One was compact barrier film adjacent to the metal and another was an outer strongly hydrated film [32]. Ellipsometric study indicated a more compact anodic film in contact with metal with a layer of $Fe(OH)_2$ and an outer more open $HFeO_2^-$ [33].

Alkali metal cations had an active role in the duplex passive film growth. The cations Li^+, K^+, Na^+ did not affect the inner layer but affected the outer layer [34]. Li, Cs^+, NH_4^+ hindered the growth rate while K^+ and Na^+ promoted the growth rate.

On anodic polarization the OH^- ions move towards film/solution interface:

$$[OH^-]_{Bulk} \rightarrow [OH^-]_{surface}$$

Depending on the local electric field and thickness, diffusion of OH^- ions from the surface to some site in the interior of the film as

$$[OH^-]_{surface} \rightarrow [OH^-]_{interior}$$

On oxidation, $Fe(OH)_2$ releases a proton as

$$Fe(OH)_2 + H_2O \rightarrow Fe(OH)_3 + H^+ + e^-$$

The proton released from the interior of the film diffuses to a site where it combines with OH^- ions to form water:

$$[H^+]_{neutralization} + [OH^-]_{neutralization} \rightarrow [H_2O]$$

As the oxidation precedes neutralization site moves towards the solution side and the progress ceases as it reached the solution phase.

3.2. *Role of anions*

The second anodic peak potential at −600 mV and the cathodic peak potential at −1030 mV varied with halide ion concentration.

$$\Delta E_p = \text{peak potential separation} = E_{p,a\,(II)} - E_{p,c\,(I)}$$

was found to vary with log halide ion concentration in all NaOH solutions. This suggests that halide participate in the film formation and growth (Figs. 5–7). ΔE_p was found to vary greatly in lower alkali solutions or when the halide ion concentrations were appreciable. Table 1 presents the variation of $i_{p,a\,(II)}$ with halide ion concentration in all NaOH solutions. In presence of halides peak currents decreased. As the metal dissolved Fe(II) ion is concentrated at the electrode surface, iron hydroxo complexes and their polymers may be formed in the interfacial diffusion layer. These metal complex ions and polymer ions are less mobile than simply hydrated ions and may provide in alkali solutions the immobile negative charge which played the ion selective role similar to the fixed charge on ion selective membranes. With progress in polymerization of metal hydroxo complexes, a precipitate layer of metal hydroxide may be formed which is cation selective. As the metal dissolution occurs current is increased the adsorption of anions, halides, on the layer covered with cations like Na^+ and Fe^{2+} ions. Consequently the diffusion layer turns to be a bipolar ion selective layer consisting of a cation selective outer sublayer originally present and an anion selective inner sublayer.

In the case of the cation selective diffusion layer the fixed charge is negative in the initial stage. With increasing dissolution current density the dissolved ferrous ion is further concentrated at the interface providing the positive fixed charge in an inner part of the interfacial diffusion layer. Then the diffusion layer turns into a bipolar ion selective layer consisting of an anion, a selective inner sublayer to the metal side and a cation selective outer sublayer to the solution side. Such a bipolar diffusion is resistive ferrous ion transport, the reverse bipolarity to anodic current and hardly allows the Fe(II) ions transport to take place unless polarized intensively. In the presence of halides at all NaOH concentrations there were decrease in anodic peak currents (Table 1). Role of anions on the dissolution, passivation and pitting was reviewed recently [35].

4. Conclusion

Hence, the oxidation of iron on cyclic polarization may take place as

$$\begin{aligned}
&\mathrm{Fe} + \mathrm{OH}^- = \mathrm{FeOH}_{\mathrm{ads}} + \mathrm{e}^-,\\
&FeOH_{\mathrm{ads}} = (\mathrm{FeOH}_{\mathrm{ads}})^+ + \mathrm{e}^-,\\
&Fe(OH)_2 + 2\mathrm{OH}^- \rightarrow \mathrm{FeOOH} + \mathrm{H_2O} + 2\mathrm{e}^-,\\
&2FeOOH = Fe_2\mathrm{O}_3 + \mathrm{H_2O}
\end{aligned}$$

At higher anodic potentials an intense electric field is induced at the boundary region between the outer and the inner sublayers. This causes dehydration and deprotonation of the bipolar layer:

$$\begin{aligned}
&\mathrm{Fe} + \mathrm{OH}^- = \mathrm{FeOH}_{\mathrm{ads}} + \mathrm{e}^-,\\
&FeOH_{\mathrm{ads}} + \mathrm{X}^- = \mathrm{Fe(X)(OH^-)} + \mathrm{e}^-,\\
&Fe(X)(OH^-) + \mathrm{X}^- \rightarrow \mathrm{FeX_2} + \mathrm{OH}^-
\end{aligned}$$

where X^- is halide ion. Conversion of salt film to oxide film without changing the oxidation state occurs:

$$\mathrm{FeX_2} + 2\mathrm{OH}^- \rightarrow \mathrm{Fe(OH)_2} + 2\mathrm{X}^-$$

and

$$\mathrm{Fe(X)_2} + 2\mathrm{H_2O} \rightarrow \mathrm{FeOOH} + 2\mathrm{X}^- + 3\mathrm{H}^+ + \mathrm{e}^-$$

at higher potentials:

$$2\mathrm{FeOOH} \rightarrow \mathrm{Fe_2O_3} + \mathrm{H_2O}$$

In alkali solutions, on anodic polarization, iron forms hydroxo complexes and their polymers in the interfacial diffusion layer. With progress of time they form a cation selective layer. In presence of halides the diffusion layer turns into bipolar ion selective layer consists of anions, a selective inner sublayer to the metal side and cation selective outer layer to the solution side. At very high anodic potentials dehydration and deprotonation lead to the conversion of salt layer to oxide.

References

[1] S. Licht, B. Wang, S. Ghosh, Science 285 (1999) 1039.
[2] I. Nowik, R.H. Herber, M. Koltypin, D. Aurbachb, S. Licht, J. Phys. Chem. Solids 66 (2005) 1307.
[3] S. Licht, B. Wang, S. Ghosh, J. Li, R. Tel-Vered, Electrochem. Commun. 2 (2000) 535.
[4] S. Licht, R. Tel-Vered, L. Halperin, Electrochem. Commun. 4 (2002) 933.
[5] M.D. Johnson, K.D. Sharma, Inorg. Chim. Acta 293 (1999) 229.
[6] R.Y.N. Ho, W. Nam, J.S. Valentine, J. Inorg. Biochem. 51 (1993) 280.
[7] S.T. Amaral, I.L. Muller, Corros. Sci. 41 (1999) 759–771.
[8] J.R. Vilche, A.J. Arvia, Anal. Acad. Nac. Cs. Ex. Fis. Nat. 33 (1981) 100.
[9] D.M. Drazic, C.S. Chao, Electrochim. Acta 27 (1982) 1409.
[10] J. Zou, D. Chin, Electrochim. Acta 33 (1988) 477.
[11] J. Zou, D. Chin, Electrochim. Acta 332 (1987) 1751.
[12] J. Flis, H. Oranowska, Z. Szklarska-Smialowska (Corros. Sci.) 30 (1990) 1085.
[13] R.D. Armstrong, I. Baurhoo, J. Electroanal. Chem. Interfacial Electrochem. 34 (1972) 41.
[14] D.D. MacDonald, D. Owen, J. Electrochem. Soc. 123 (1976) 824.
[15] D.D. MacDonald, B. Roberts, Electrochim. Acta 23 (1978) 557.
[16] D.D. MacDonald, B. Roberts, Electrochim. Acta 23 (1978) 7811.
[17] G.T. Burstein, G.M. Ashley, Corrosion 39 (1983) 241.
[18] J.O. Zerbino, J.R. Vilche, A.J. Arvia, J. Appl. Electrochem. 11 (1981) 703.
[19] M. Jayalakshmi, V.S. Muralidharan, Corros. Rev. 12 (1994) 305.
[20] R.S. Schrebler-Guzman, J.R. Vilche, A.J. Arvia, Electrochim. Acta 24 (1979) 395.
[21] R.S. Schrebler-Guzman, J.R. Vilche, A.J. Arvia, J. Appl. Electrochem. 11 (1981) 551.
[22] D. MacDonald, B. Roberts, Electrochim. Acta 23 (1978) 781.
[23] D. Geana, A.A. Ei Miligy, W.J. Lorenz, J. Appl. Electrochem. 4 (1974) 337.
[24] G. Kreysa, B. Hakansson, Electrochim. Acta 23 (1978) 61.
[25] B. Anderson, I. Ojefers, J. Electrochem. Soc. 123 (1979) 824.
[26] L.D. Burke, M.E.G. Lyons, J. Electroanal. Chem. 198 (1986) 347.
[27] H. Noblich, D. Groppel, W. Nippe, F.V. Sturn, Chem. Eng. Technol. 45 (1973) 203.
[28] V.S. Muralidharan, M. Veerashunmugamani, J. Appl. Electrochem. 15 (1985) 675.
[29] E.B. Eronko, A.V. Bogdanov, I.A. Shoshina, T.K. Teplunskay, A.L. Rotinyan, Zh. Rikl. Khim. 59 (1986) 1011.
[30] D.W. Shoesmith, P. Taylor, M.G. Bailey, B. Ikeola, Electrochim. Acta 23 (1978) 903.
[31] O.A. Albani, J.O. Zerbino, J.R. Vilche, A.J. Arvia, Electrochim. Acta 31 (1986) 1403.
[32] N. Sato, K. Kudo, R. Nishi Mura, J. Electrochem. Soc. 123 (1976) 1419.
[33] N. Sato, T. Nado, K. Kudo, Electrochim. Acta 19 (1974) 471.
[34] S. Juanto, R.S. Schrebler, J.O. Zerbino, J.R. Vilche, A.J. Arvia, Electrochim. Acta 36 (1991) 1143.
[35] V.S. Muralidharan, Corros. Rev. 21 (4) (2003) 327.